climate

MDPI

Article

A 133-Year Record of Climate Change and Variability from Sheffield, England

Thomas E. Cropper [1,*] and Paul E. Cropper [2]

[1] School of Earth and Ocean Sciences, Cardiff University, Wales CF10 3AT, UK
[2] Rhodium Tutoring, Sheffield S8 8QW, UK; pc@rhodiumts.co.uk
* Correspondence: CropperT@Cardiff.ac.uk or thomascropper@outlook.com

Academic Editor: Christina Anagnostopoulou
Received: 8 May 2016; Accepted: 5 September 2016; Published: 14 September 2016

Abstract: A 133-year length (1883–2015) daily climate record from Sheffield, England (53.38°N, 1.49°W) is analysed. Across the entire length of the record, there are significant warming trends annually and for all seasons, whereas precipitation shows a significant annual increase but the seasonal trends, whilst all positive, are not significant. Trends in extreme indices mirror the mean long-term warming and wetting signal. Record hot and cold daily temperatures and precipitation amounts are associated with summer anticyclonic conditions, an anomalous easterly winter jet stream and summer cyclonic activity, respectively. Whilst there are large uncertainties surrounding the calculation of return periods for the daily maximum, minimum and precipitation records from a single record, our best estimates suggest that in the current climate (2015), the existing records have return periods of 38, 529 and 252 years, respectively. The influence of several climate indices on mean and extreme indices are considered on seasonal scales, with the North Atlantic Oscillation displaying the strongest relationship. Future mean maximum temperature and precipitation alongside extreme indices representing the warmest and wettest day of the year are analysed from two downscaled climate model output archives under analysis periods of a 1.5 and 2 degree warmer world and the 2080–2099 end of 21st century period. For this mid-latitude location, there is minimal difference in model projections between a 1.5 and 2 degree world, but a significant difference between the 1.5/2 degree world and the end of century 2080–2099 period under the most severe climate warming scenarios.

Keywords: climate; Sheffield; extremes; global warming; cmip5; temperature; precipitation

1. Introduction

During the last decade, several unusual and extreme weather events and periods have occurred across the United Kingdom (UK). The record breaking Yorkshire floods of June 2007 [1,2] marked the first of six consecutive years in a row with above average summer precipitation across northern Europe [3]. Within this six-year period of enhanced summer precipitation, central, eastern and southern England and Wales experienced a significant drought during 2010–2012, which was subsequently ended by the wettest April–June period for England and Wales in 250 years [4]. Significant snow events occurred across the UK during the winters of 2009–2010, 2010–2011 and March 2013 [5–7]. The stormy winter of 2013–2014 was the wettest winter on record for the UK [8] and this was followed by the second wettest winter and warmest December on record during the 2015–2016 winter [9]. Conversely, 2014 was the warmest year in the Central England Temperature record [10]. Since the end of the 20th century there have been a greater proportion of warm and wet UK climate records broken and much fewer cold and dry records broken [11]. The clustering of these recent unusual and extreme phenomena raises the question of whether or not UK weather extremes are significantly responding to

anthropogenic global warming, or whether natural variability is the dominant force in a geographic location with highly variable intra-seasonal weather and climate conditions.

One way to place recent variability into context is analysis of long-term, daily temporal resolution, high quality climate time-series. Uninterrupted, daily weather observations, with minimal gaps, have been taken at Weston Park (hereafter "WP", 53.38°N, 1.49°W, Figure 1), Sheffield, England, since 5 September 1882. The purpose of this paper is to present an analysis of the climate changes and weather records that have been observed at WP from 1883 until the end of 2015, to discuss and place these changes into context and to examine the potential future evolution of extreme precipitation and temperatures for Sheffield.

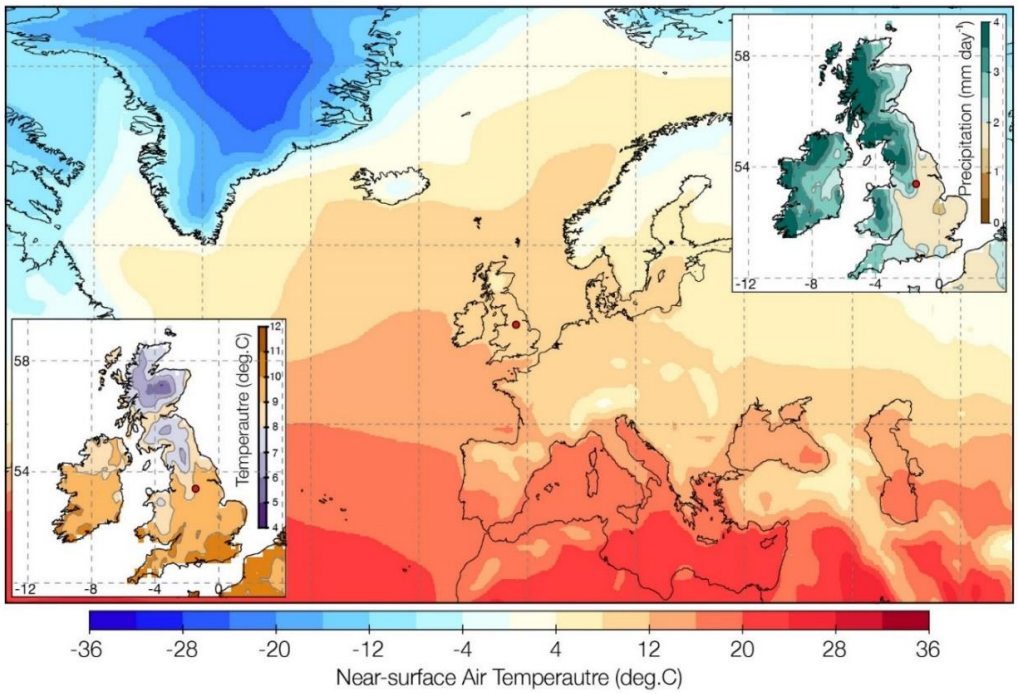

Figure 1. The mean annual temperature (1979–2015) at 2 m height (above land) and sea-surface temperature (above oceans) from the ERA-Interim Reanalysis [12]. Inset plots show the mean annual temperature and precipitation (1950–2015) from the E-OBS dataset [13] focused on the UK. The location of WP is indicated by a red marker in all panels. Plot units are degrees Celsius and mm day^{-1}.

2. Materials and Methods

Daily weather observations of maximum/minimum temperatures (TX/TN) and precipitation have been taken at ~09:00 GMT at WP since 5 September 1882. The WP station underwent two very minor location changes in 1920 and 1951. During 2003–2006, automated equipment was introduced alongside the traditional precipitation gauge and maximum/minimum thermometers. During these years, measurements were taken simultaneously using the manual and automatic instruments to ensure consistency. Since 2010, the WP data are from the automated equipment and the data undergo a rigorous initial quality control procedure [14] before being archived. Gaps in TX and TN were filled according to the following:

1. If the gap was one day, the value was interpolated between the previous and following day.
2. If the gap was greater than one day, and the corresponding TX/TN value was present, then the missing value was set to the 11-year average of the TX/TN difference equal to the daily diurnal temperature range (DTR) of the missing day.
3. If both TX and TN were missing for more than one day, the values were set to the 11-year daily average of the missing days.

We use an 11-year average above so that interpolated values are the average of the decadal climate at the time the data are in-filled. In total, there were seven days when both TX and TN were missing, out of a total of 45 (79) missing days for TX (TN). There were 1545 days when trace precipitation was recorded, which was set to 0 mm, and four days in November 1903 when precipitation was recorded, but no value was given. With no realistic way of determining the exact amount of precipitation on these days, we gave each day a value of 0.2 mm (arbitrarily set, as we assume the day had "rain", so use 0.2 mm as this exceeds the 0.1 mm threshold used in the calculation of a precipitation index used in our analysis (Table 1)). After gap filling, we considered the period January 1883–December 2015 for our analysis, giving a complete time-series of 48,577 days. In addition to standard analysis methods, we also applied extreme indices analysis on the daily WP data using the Expert Team on Climate Change Detection and Indices (ETCCDI, Table 1). Indices are calculated using the RCLIMDEX software [15] setting the base period to 1951–2005. There are four distinct classes of indices: "absolute", "threshold", "duration" and "percentile". Absolute indices are based on a physically relevant temperature value (e.g., the lowest value of the minimum temperature recorded in a year/season). Threshold indices are when either the daily maximum or minimum temperature surpasses or falls below a set value, and percentile indices are similar to threshold indices, but the threshold value is drawn from a chosen climatological percentile for each day. Duration indices count the number of days where a value (either a set threshold or daily percentile) is exceeded. For trend analysis via linear regression, we use the Theil-Sen slope estimator, with the significance of trends estimated using the modified Mann-Kendall trend test [16]. To supplement our main methods we also apply quantile regression analysis to daily precipitation data in Section 3.3, extreme value analysis to daily climate records and analyse climate model output in Section 3.4.

Table 1. The ETCCDI indices used in this study. The Tropical Nights index has been altered from the standard 20 °C (TR20) to 15 °C here (TR15) which is more suitable for the climate of WP.

Long Name	Index Name	Definition	Units
Summer Days	SU25	Frequency of daily maximum temperature > 25 °C	Days
Tropical Nights	TR15	Frequency of daily minimum temperature > 15 °C	Days
Frost Days	FD	Frequency of daily minimum temperature > 0 °C	Days
Growing Season Length	GSL	Number of days where the mean temperature is > 5 °C for six consecutive days after January 1st and < 5 °C for 6 consecutive days after July 1st	Days
Warmest TX	TXx	Value of the maximum daily maximum temperature	°C
Coldest TX	TXn	Value of the minimum daily maximum temperature	°C
Warmest TN	TNx	Value of the maximum daily minimum temperature	°C
Coldest TN	TNn	Value of the minimum daily minimum temperature	°C
Warm Days	TX90p	Days when the daily maximum temperature is above the 90th percentile for that day	Days (%)
Cold Days	TX10p	Days when the daily maximum temperature is below the 10th percentile for that day	Days (%)
Cold Nights	TN10p	Days when the daily minimum temperature is below the 10th percentile for that day	Days (%)
Warm Nights	TN90p	Days when the daily minimum temperature is above the 90th percentile for that day	Days (%)
Warm Spell Duration Indicator	WSDI	Number of days when the daily maximum temperature exceeds the daily 90th percentile (minimum of six days for a period to be counted)	Days
Cold Spell Duration Indicator	CSDI	Number of days when the daily minimum temperature is below the daily 10th percentile (minimum of six days for a period to be counted)	Days
Diurnal Temperature Range	DTR	Average difference between daily maximum and minimum temperatures	°C
Simple Daily Intensity Index	SDII	Ratio of annual total precipitation to the number of wet days (>1 mm)	mm day^{-1}

Table 1. *Cont.*

Long Name	Index Name	Definition	Units
Wettest consecutive five days	RX5day	Maximum of consecutive five day precipitation	mm
Wettest day	RX1day	Maximum daily precipitation	mm
Heavy precipitation days	R10m	Number of days where precipitation > 10 mm	Days
Very heavy precipitation days	R20m	Number of days where precipitation > 20 mm	Days
Precipitation from very wet days	R95p	Amount of precipitation from days > 95th percentile	mm
Precipitation from extremely wet days	R99p	Amount of precipitation from days > 99th percentile	mm
Consecutive Wet Days	CWD	Maximum number of consecutive days when precipitation > 1 mm	Days
Consecutive Dry Days	CDD	Maximum number of consecutive days when precipitation < 1 mm	Days

3. Results

3.1. Mean

Figure 1 displays the location of WP and illustrates that in terms of the annual climatology, WP is situated in the boundary between the warmer, drier, southeast and colder, wetter, northwest of England. Figure 2 shows the annual cycle from WP for TX, TN and precipitation. Monthly mean data and climate records are given in Tables 2–4, time series for mean temperature and precipitation are shown in Figure 3 and trend rates for various periods for mean temperature, TX, TN and precipitation are given in Table 5. January is the coldest month and July the warmest month (Figure 2; Table 3), but eight out of ten extreme hot records were found during August or September, rather than July (Table 2). December (monthly) and winter (seasonally) have the greatest precipitation amounts. The standout feature in Figure 2c is the impact of individual large summer precipitation events on the daily standard deviation and maximum daily precipitation amounts (Figure 2; Table 2). The mean value for the daily maximum precipitation amount across the nine non-summer months is 26.8 mm, whereas for the three summer months this is 35.1 mm. The chance of precipitation (i.e., a day with >=0.1 mm) on a given calendar day averages 52.5% across the entire record; there is a seasonal cycle with higher probabilities of precipitation in autumn and winter, and the lowest and highest daily values range from 35.6% (29 May) to 73.5% (3 November).

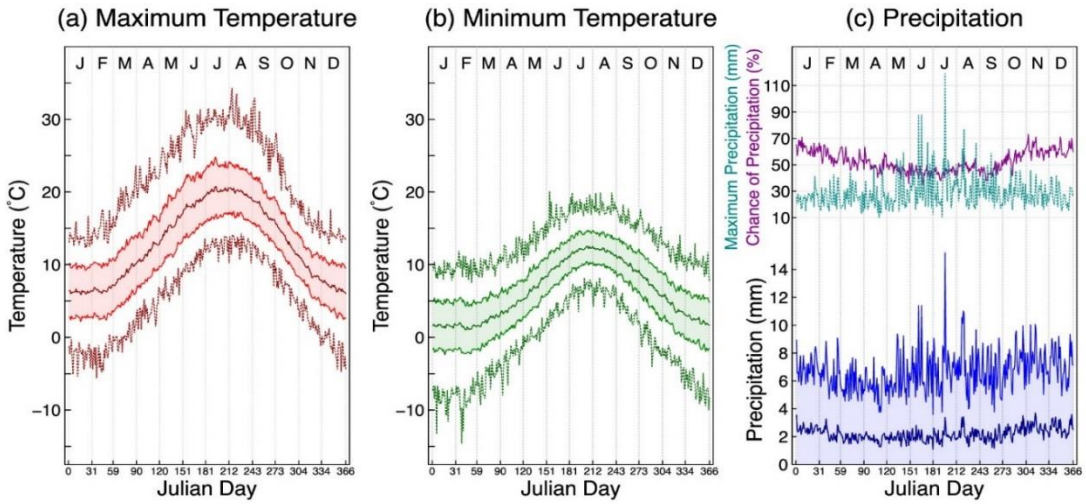

Figure 2. (**a**,**b**) The 1883–2015 daily mean TX/TN (main bold line). Shaded regions indicate ±1 standard deviation and outlying lines indicate the record maximum/minimum daily value. (**c**) The lower plot indicates the daily mean (bold line) and standard deviation (shaded region) of precipitation. The upper axis illustrates the daily maximum recorded precipitation value and the daily likelihood of precipitation (same scale, but units of mm for maximum precipitation and per cent for precipitation likelihood).

Table 2. The top ten record days for precipitation, TX and TN. Units in °C and mm.

Rank	Date	TX	Rank	Date	TN	Rank	Date	Precipitation
1	03/08/1990	34.3	1	08/02/1895	−14.6	1	15/07/1973	119.2
2	09/08/1911	33.5	2	06/01/1894	−13.3	2	14/06/2007	88.2
3	02/08/1990	33.4	3	10/02/1895	−12.9	3	10/06/2009	88.1
4	02/09/1906	32.9	4	21/01/1940	−11.6	4	09/08/2004	77
5	01/09/1906	32.8	5=	18/01/1891	−10.7	5	22/06/1982	66.6
6	01/07/2015	32.7	5=	19/01/1891	−10.7	6	25/08/1986	66.5
7	08/08/1975	32.6	7=	06/02/1895	−10	7	07/08/1922	62.1
8=	09/08/1975	32.3	7=	30/12/1908	−10	8	30/06/2003	60.9
8=	31/08/1906	32.3	9=	07/02/1895	−9.7	9	21/05/1932	59.4
10	31/07/1943	31.8	9=	09/02/1895	−9.7	10	14/09/1994	58.9
			9=	14/02/1929	−9.7			

Since the turn of the 21st century, four out of the top ten daily precipitation records have been set but only one extreme warm or cold temperature record has occurred: the sixth warmest day on record, on 1 July 2015 (Table 2). The year 2011 is the warmest year in the WP record (Table 4) and a clear generalised warming trend is evident in the annual mean temperature time series (Figure 3). Trend analysis (Table 5) indicates that for the long term 1883–2015 record, all annual and seasonal trends in mean temperature, TX and TN are statistically significant, ranging from 0.47 to 1.35 °C·century^{-1}. Spring is the season with the strongest mean warming signal (1.28 °C·century^{-1}) and the annual, summer and autumn rates are all close to 1 °C·century^{-1} but the winter season has experienced a warming rate only about half that of the other seasons at 0.58 °C·century^{-1}. For other periods, trend direction and significance are not as ubiquitous. Examples include winter during 1901–2000 where the trend direction is negative, but only very marginally and not significantly so, and throughout the 1941–1970 period across all seasons. For the periods towards the end of the record (1961–1990, 1971–2000, 1981–2010, and 1991–2014), all seasonal and annual mean temperature, TX, and TN trends are positive, but trend significance is not widespread. Annual precipitation throughout the entire record is significantly increasing at a rate of 68.6 mm·century^{-1} (Table 5; Figure 3), which with the exception of autumn precipitation during 1941–1970, is the only significant precipitation increase in the WP record.

Out of the five driest/wettest, and coldest/warmest months, seasons and years (Table 4), December 2010 and March 2013 are the only months since the turn of the 21st century which display a cold record. Record warm months/seasons/years since the turn of the 21st century appear more common, although February, May and August have not had a post-2001 record warm month, but all other months and seasons have at least one out of five record months/seasons. Only four months (January 2006, March 2011, April 2007 and December 2010) and one season (spring 2011) have experienced a record dry month, however 2003 and 2011 feature as the fifth and third driest years on record, respectively. Conversely, 2012 and 2002 are the first and third wettest years on record, respectively and June (summer) has seen three out of five (two out of five) record wettest months (seasons) since the turn of the century.

Table 3. The monthly, seasonal and annual mean temperature and precipitation total for the weather station at WP, 1883–2015 (standard deviation in brackets).

	Jan	Feb	Mar	Apr	May	Jun	Jul	Aug	Sep	Oct	Nov	Dec	ANN	DJF	MAM	JJA	SON
Temperature	3.9 (1.6)	4.0 (1.9)	5.7 (1.7)	8.1 (1.3)	11.2 (1.2)	14.3 (1.1)	16.1 (1.3)	15.8 (1.3)	13.6 (1.1)	10.1 (1.3)	6.6 (1.2)	4.6 (1.6)	9.5 (0.7)	4.2 (1.2)	8.3 (1.0)	15.4 (0.9)	10.1 (0.9)
Precipitation	79.6 (37.2)	63.3 (38.5)	59.2 (31.1)	55.0 (31.0)	59.5 (31.4)	58.1 (42.0)	62.6 (36.2)	68.0 (35.9)	57.9 (37.5)	75.9 (38.6)	78.9 (40.1)	82.7 (41.4)	800.8 (122.6)	225.8 (74.4)	173.7 (56.0)	188.7 (70.3)	212.7 (66.6)

Table 4. The five-coldest/warmest and driest/wettest months, seasons and years based on mean temperature and precipitation data. Years since 2001 are highlighted to indicate "recent" (post-20th century) records.

	Driest–5th Driest					5th Wettest–Wettest					Coldest–5th Coldest					5th Warmest–Warmest				
Jan	1997	**2006**	1989	1953	1888	1984	1948	1928	1988	1986	1940	1963	1895	1979	1941	1983	1921	**2007**	1898	1916
Feb	1891	1959	1985	1998	1895	1950	1923	1966	**2002**	1977	1947	1895	1986	1963	1929	1914	1961	1990	1945	1998
Mar	1929	1931	1938	1944	**2011**	1916	1941	1947	1979	1981	1883	**2013**	1969	1888	1916	1990	1957	1961	**2012**	1938
Apr	1957	1938	**2007**	1954	1984	1983	1920	1966	2000	**2012**	1917	1922	1891	1986	1908	1987	**2014**	1943	**2007**	**2011**
May	1935	1905	1896	1956	1991	**2014**	1983	1932	1967	1886	1902	1894	1885	1887	1923	1989	1952	1964	1947	1992
Jun	1925	1941	1889	1983	1921	1998	**2012**	**2009**	1982	**2007**	1916	1909	1927	1923	1991	**2003**	1960	**2006**	1940	1976
Jul	1911	1977	1921	1979	1984	**2002**	1956	1958	1930	1973	1888	1892	1922	1907	1919	1976	**2013**	1995	1983	**2006**
Aug	1940	1991	1933	1995	1947	1931	1956	1954	**2004**	1922	1912	1885	1986	1922	1956	1990	1947	1997	1995	1975
Sep	1959	1928	1910	1941	1986	1883	1994	1968	1965	1918	1952	1912	1918	1894	1925	1929	1999	1895	1949	**2006**
Oct	1978	1947	1972	1904	1888	**2002**	1885	1960	1903	1998	1896	1892	1885	1887	1905	1995	1969	**2005**	**2001**	1921
Nov	1945	1958	1909	1889	1956	1969	2000	1954	1940	1951	1919	1910	1915	1923	1985	1899	1938	**2015**	1994	**2011**
Dec	1933	1905	1890	1963	**2010**	1993	1929	1915	1978	1965	1890	1981	**2010**	1927	1950	1898	1974	1988	1934	**2015**
DJF	1964	1891	1934	1932	1929	1916	1984	1977	1990	1966	1963	1947	1979	1895	1940	1975	1935	1998	**2007**	1989
MAM	**2011**	1990	1938	1929	1957	1889	1886	1983	1981	1979	1891	1887	1888	1941	1883	1990	**2007**	**2014**	1945	**2011**
JJA	1995	1976	1887	1959	1983	1931	**2012**	1956	1912	**2007**	1888	1907	1922	1892	1902	1995	1933	**2003**	**2006**	1976
SON	1975	1884	1904	1948	1964	1944	1965	1935	1960	2000	1887	1919	1952	1993	1885	1959	**2014**	1978	**2011**	**2006**
ANN	1887	1975	**2011**	1921	**2003**	1960	1965	**2002**	2000	**2012**	1892	1888	1885	1891	1919	1959	1990	**2006**	**2014**	**2011**

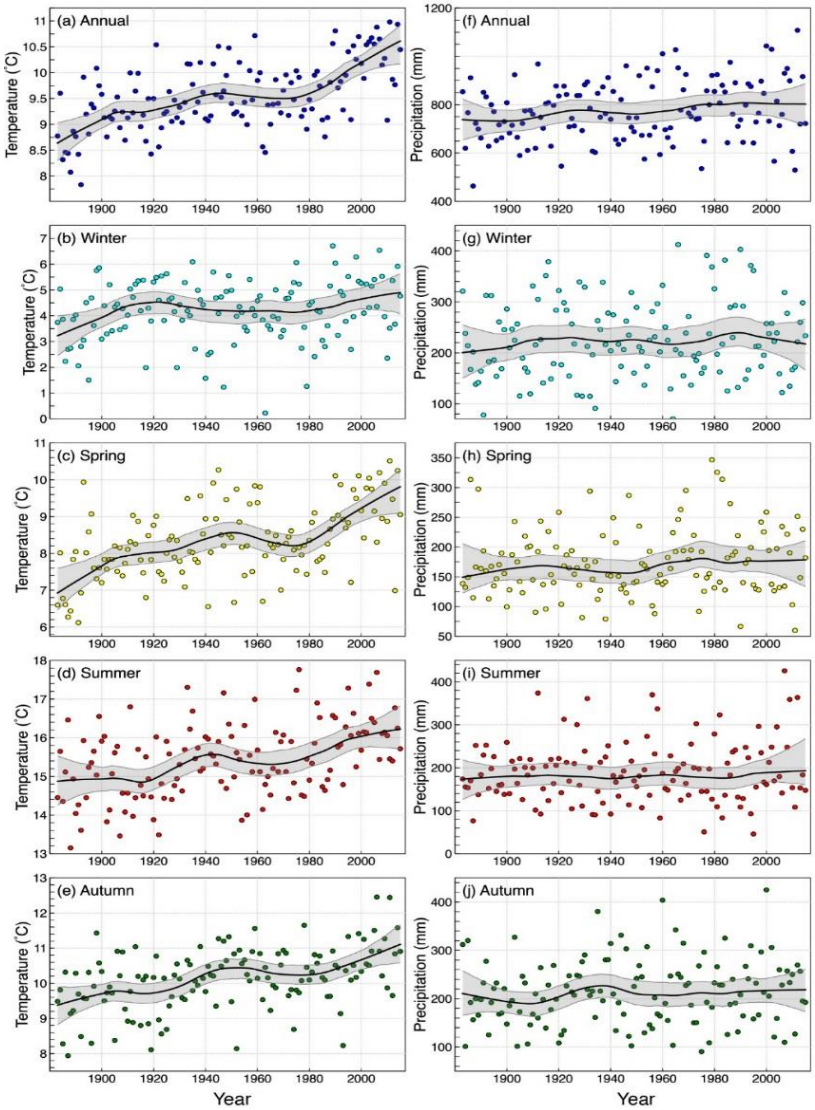

Figure 3. The seasonal and annual evolution of (**a**–**e**) mean temperature and (**f**–**j**) total precipitation from WP, 1883–2015. Locally-weighted regression trends ($n/2$ smoothing parameter) with 95% confidence intervals are plotted for each panel.

Table 5. Trend rates in mean temperature, TX, TN and precipitation for standard climate periods as in [17,18] (°C, Days, % or mm per century for 1883–2015 and 1901–2000, per decade for other periods). Bold values indicate trend significance ($p < 0.05$).

Period	Mean Temperature					Maximum Temperature					Minimum Temperature					Precipitation				
	ANN	DJF	MAM	JJA	SON	ANN	DJF	MAM	JJA	SON	ANN	DJF	MAM	JJA	SON	ANN	DJF	MAM	JJA	SON
1883–2015	**1.00**	**0.58**	**1.28**	**1.03**	**0.96**	**1.00**	**0.62**	**1.35**	**1.06**	**1.00**	**0.94**	**0.47**	**1.25**	**1.02**	**0.96**	**68.64**	14.72	12.97	8.60	19.42
1901–2000	**0.69**	−0.02	**0.85**	**1.06**	**0.70**	**0.74**	0.08	**0.79**	**1.20**	**0.80**	**0.62**	−0.14	**0.84**	**0.84**	**0.72**	80.39	13.39	18.35	−9.72	29.20
1931–1960	0.04	−0.04	0.27	−0.15	0.26	0.04	0.00	0.27	−0.21	0.27	0.06	−0.05	0.22	−0.06	0.18	6.75	14.52	−8.72	15.78	−14.41
1941–1970	−0.10	−0.29	−0.24	−0.14	−0.07	−0.14	−0.27	−0.32	−0.15	−0.03	−0.09	−0.18	−0.18	−0.08	−0.11	31.00	2.77	18.73	−0.75	**17.50**
1951–1980	0.00	0.18	−0.17	0.07	−0.17	0.01	0.10	−0.19	0.07	−0.15	−0.03	0.25	−0.14	0.00	−0.18	20.64	10.77	4.33	−4.86	-8.28
1961–1990	0.20	0.30	0.13	**0.26**	0.06	**0.26**	0.37	0.19	0.32	0.11	0.09	0.21	0.03	**0.19**	0.06	20.64	23.92	−4.58	−4.86	−8.78
1971–2000	**0.27**	0.19	**0.49**	**0.32**	0.18	**0.32**	0.38	**0.51**	**0.36**	0.12	0.21	0.05	**0.38**	**0.25**	**0.19**	24.00	11.71	2.11	−11.58	27.29
1981–2010	**0.35**	0.37	**0.45**	**0.29**	0.23	0.32	0.35	**0.53**	0.24	0.19	**0.38**	0.39	**0.39**	**0.36**	**0.29**	−4.00	−7.75	−12.00	28.67	1.00
1991–2015	0.28	0.20	0.16	0.06	0.44	0.22	0.00	0.19	-0.09	0.49	**0.35**	0.32	0.09	0.21	**0.52**	10.66	2.00	1.73	13.13	−9.62

Table 6. As for Table 5 but for ETCCDI climate indices (Table 1). (°C, Days, % or mm per century for 1883–2015 and 1901–2000, per decade for other periods). Trends for CSDI and WSDI have been excluded here as they are neutral for all time periods. Bold values indicate trend significance ($p < 0.05$).

Period	DTR	SU25	TR15	FD	GSL	TXx	TXn	TNx	TNn	TX90p	TX10p	TN10p	TN90p	SDII	RX5Day	Rx1Day	R10mm	R20mm	R95p	R99p	CWD	CDD
1883–2015	0.05	**2.2**	**4.9**	−8.7	**25.1**	**1.2**	**1.0**	**1.3**	**1.3**	**4.1**	**−7.2**	**−6.3**	**5.3**	**0.40**	8.3	6.2	2.7	0	28.9	0	0	−1.6
1901–2000	0.15	**3.5**	**3.7**	0	**11.0**	1.0	0.5	**1.3**	**0.6**	**4.6**	**−5.1**	**−4.3**	**3.9**	**0.56**	**14.7**	**9.4**	**4.5**	**1.5**	**56.9**	**1.6**	0	0
1931–1960	0	−0.4	−0.9	0	10.0	−0.2	0	0	0.1	0.4	−0.1	−0.4	0	0	0.3	0.9	1.5	0	−8.3	0	0	0
1941–1970	0	−0.7	−1.3	3.2	3.3	**−0.8**	0.3	−0.1	−0.3	−0.4	0.2	0.3	−1.0	−0.1	0.6	**4.2**	0	0	12.5	7.8	0	−1.9
1951–1980	0.01	1.4	0	0	−7.5	0.1	0.1	−0.1	0.3	1.3	0.4	−0.5	−0.2	0	2.7	3.2	−0.7	0.4	18.5	8.0	0.5	0.8
1961–1990	0.13	2.1	**2.0**	−2.9	−5.7	1.0	0.6	0.3	0.8	**2.4**	**−2.3**	−0.7	**1.4**	0.3	6.7	1.9	2.0	**0.8**	12	−0.3	0	1.1
1971–2000	0.12	1.5	1.7	0	11.7	**1.0**	0.4	0.3	0.2	1.3	**−1.5**	−0.4	**1.6**	0.1	−0.1	−1.4	**2.4**	0	2.1	−1.2	0.7	−2.0
1981–2010	−0.10	−0.4	2.6	**−4.3**	13.8	0.2	0.2	0.3	0.6	0	**−1.8**	**−1.7**	**2.1**	−0.1	0.5	2.5	−0.6	**−1.0**	−23.6	8.0	0	−1.0
1991–2015	−0.10	−1.1	1.4	−6.2	12.3	0.2	0.4	0.1	**1.0**	0.8	**−2.4**	**−1.9**	1.1	−0.1	−4.3	−1.9	−1.8	−0.6	−31.2	−1.9	0	−1.3

3.2. Extremes

Table 6 and Figure 4 show the results from application of the ETCCDI analysis on the WP data. As with the analysis on the "base" data (i.e., mean temperature and precipitation, TX, and TN) centennial trends across the entire period and the 20th century are significant across many indices, including positive trends towards warmer or wetter conditions in the "absolute" temperature and precipitation indices (TXx, TXn, TNn, TNx, RX1Day, RX5Day and R10mm). Significant long-term increases in TX90p and TN90p and decreases in TX10p and TN10p are also indicative of warming conditions and positive trends in SDII (significant) and R95p indicate an increase in intense/heavier precipitation events (but not necessarily the frequency). The R95p, R99p and R20mm trends are positive and significant for the 20th century, but not the long-term record (1883–2015). Whilst a long term increase in all three of these series is visually inferable (Figure 4) the long-term R99p and R20mm trends are given as zero with the Theil-Sen method. With this method, if more than half of the data points in a series have a value which is the same as the preceding/following value, then the resultant trendline will be zero (as the Theil-Sen method is the median value of all possible ranked slopes). The thresholds for the 95th and 99th daily precipitation percentiles are 18.2 and 31 mm·day^{-1}, respectively. This presents a somewhat curious difference between the long-term R20mm trend and the R95p trend (29 mm·century^{-1}, Table 6), which is mainly due to the different units—R20mm requires an increase in frequency of "very heavy" precipitation days, whereas R95p does not (just the precipitation amount)—but we also find a non-trivial number of days (183) where precipitation was between the 18.2 and 20 mm threshold (relative to a count of 635 R20mm days), highlighting how careful selections must be made when determining thresholds for analysing "moderate" extreme events (i.e., ~one year return period)

To eliminate any ambiguity with regards to the trend in extreme precipitation, we supplement the analysis of the ETCCDI indices with trends in the quantiles of precipitation using quantile regression [19], which shows a clear divide between negative trends in the <80th percentiles and positive trends in the >80th percentiles (Figure S1). There is no long term change in CWD and a slight, but non-significant decrease in CDD. A significant change in these indices would require a very strong signal, given that the annual average of a daily chance of precipitation is 52.5%. With no significant change in precipitation frequency, and a strong indication of an increase in extreme precipitation (Figure 4, Figure S1), most of the increase in annual precipitation (Table 5, Figure 3) must therefore be coming from extreme precipitation events, which during the last ~35 years appears to be dominated by extreme summer precipitation events (Table 2, Table 5).

The long-term trends in the extreme indices support the findings derived from mean annual data of a generalised warming and precipitation increase. As with seasonal and annual temperature data, trend significance for shorter periods and rates for the periods at the end of the record (1961–1990, 1971–2000, 1981–2010, and 1991–2014) are rarely ubiquitously significant but generally agree on direction. Trends in SU25 and TR15 both show a long-term increase (Table 6), with 1974 and 1972, respectively, being the last years where a count of zero for both these indices was recorded (Figure 4). An increase (decrease) in the number of days in the WSDI (CSDI) is perhaps visually inferable (Figure 4) but as mentioned before, the Theil-Sen trend gives a value of zero with many consecutively equal values.

The typical weather pattern associated with extreme high and low temperatures and precipitation (using the dates from Table 2) are shown as a composite anomaly plot in Figure 5. Record hot days at WP are associated with summer anticyclone conditions centred over southern Scandinavia, which allows advection of warm continental air toward the UK. Record cold days occur under a large-scale reversal of the winter climatological pressure gradients, driving an anomalous easterly jet stream bringing cold Arctic air across most of northern Europe. Record precipitation days, which all occur during the summer months (Table 2) are driven by cyclonic conditions centred over/around the southwest of the UK. Positive Convective Available Potential Energy anomalies imply a contribution to rainfall intensity from convection enhancement (i.e., why the record precipitation values are

all during summer as opposed to other seasons), but unfortunately sub-daily precipitation data were not available for analysis, which could have provided further insight. Some hot and cold extreme records were part of the same meteorological "event", i.e., consecutive days (Table 2), so we replicated the composite analysis using subsequently ranked record days that were from unique events (not consecutive days) to remove the weighting in the composite plot from two/three specific events, but this did not markedly alter the composition of the plots (not shown).

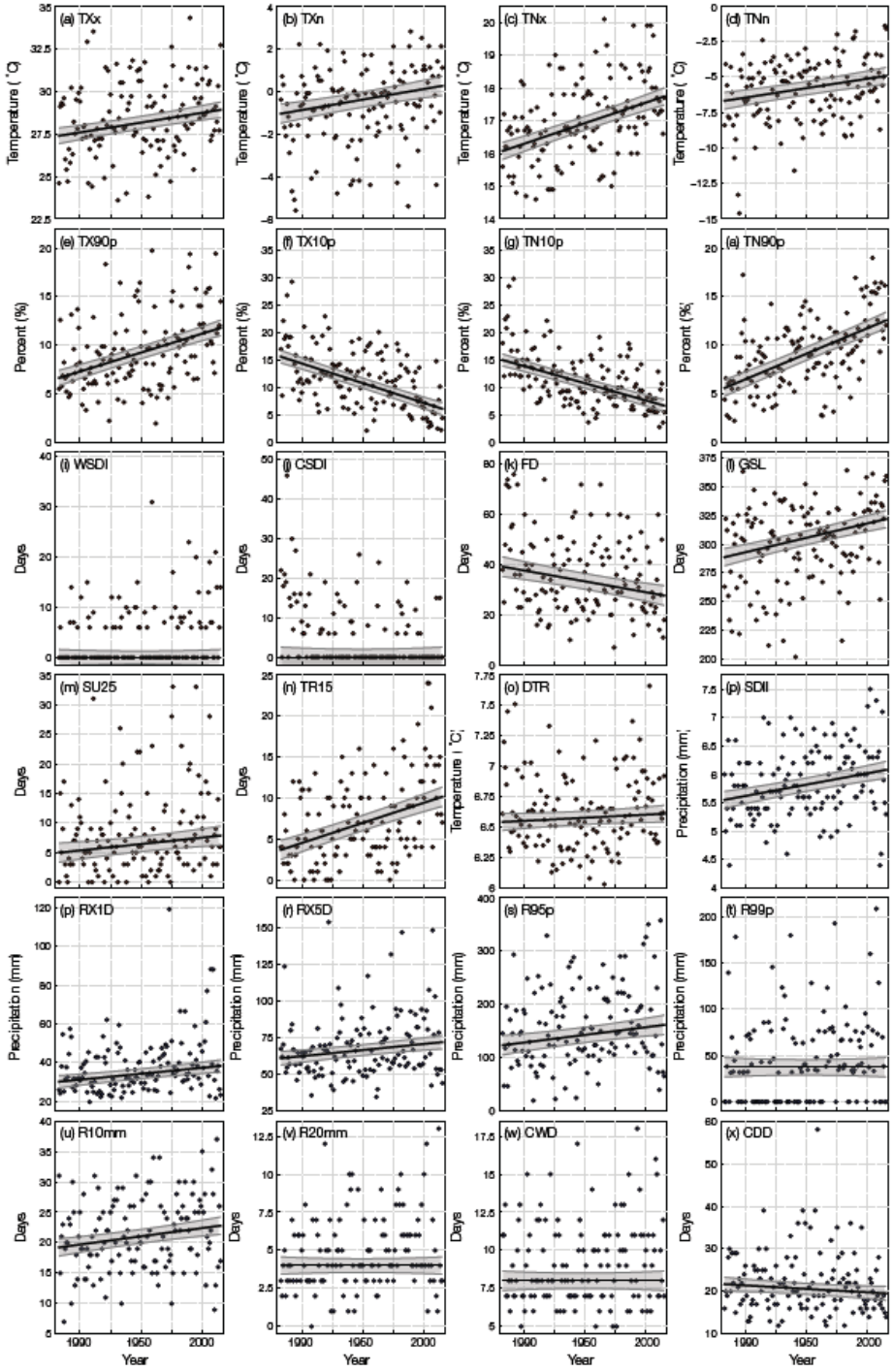

Figure 4. The annual evolution of (**a**–**x**) 24 extreme indices for WP. Solid lines are Theil-Sen trends for the period 1883–2015 with 95% confidence intervals (accounting for autocorrelation) in grey shading.

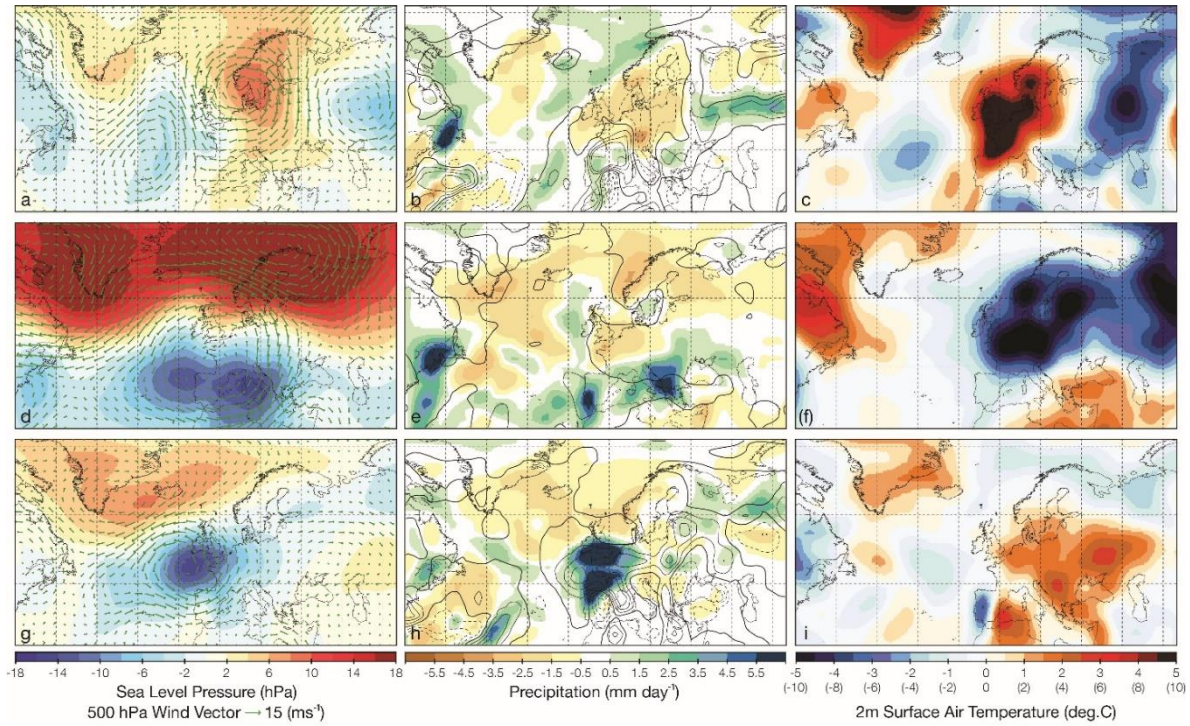

Figure 5. Composites of daily 500 hPa wind speed and direction anomalies and near-surface precipitation and mean temperature anomalies of the ten record: (**a**–**c**) TXx; (**d**–**f**) TNn; and (**g**–**i**) precipitation days. Data are from the Twentieth Century Reanalysis v2c [20] with the climatology base period as 1981–2010. One TXx record was set in 2015, outside of the reanalysis temporal period, so the 11th record value was used. Contours on plots b, e and h represent Convective Available Potential Energy anomalies, with solid (dashed) lines indicating positive (negative) anomalies at intervals of 40 J·kg^{-1}, with the zero contour enhanced. The second row of temperature anomalies for the right hand panels are the scale for plot f.

Whilst four out of the ten daily precipitation records have been set since the turn of the 21st century (Table 2), the record event on 15 July 1973 is over 30 mm higher than any other daily value. The warm (3 August 1990) and cold (8 February 1895) records are also stand-out values, exceeding the second warmest (coldest) day by 0.8 °C (1.3 °C). Seen as these events represent the extreme statistics of the WP record, each by some distance, they mark the absolute range of extremities possible in the historical WP climate. This raises two questions. Firstly, what is/was the probability of these extreme events occurring in the climate at the time and at present (2015) and is there a detectable anthropogenic component? Secondly, what their evolution might be in the future under a warming climate. Were these events exceptional and unlikely to be passed, or will future climate warming turn these records into "normal" conditions? To answer this, we take two approaches. In Section 3.4, we analyse the potential future evolution of two extreme indices, TXx and RX1day, from global climate models. Here, we analyse the three WP climate records discussed above by fitting the time series of TNn, TXx and RX1day to the Generalised Extreme Value distribution (details given in Supplementary A) with smoothed global average temperatures as a covariate [21–24]. Table 7 provides results for this analysis for return periods calculated for the climate at the time of the record and again in 2015 and the respective ratio between these for the WP record statistics and A posteriori determined "moderate" extreme values (a threshold of 75 mm, 32 °C and −8 °C for precipitation, TXx and TNn, respectively) that have an approximate return period of a decade.

Table 7. Return period and ratios between the return periods (between 2015 and the point in time which the WP record was set: 1990 for TXx, 1895 for TNn and 1973 for RX1Day) for the individual record climate values set at WP and also for posteriori determined "moderate" extreme values (a threshold of 75 mm, 32 °C and −8 °C for precipitation, TXx and TNn, respectively) with a return period of approximately a decade which have more tightly constrained 95% confidence interval estimates. * indicates the ratio has been inversed so less likely TNn events are given as positive ratios to match TXx and precipitation.

Moderately Extreme Value	Return Period (Climate at Time of Record)	Return Period (2015)	Ratio	Record Value	Return Period (Climate at Time of Record)	Return Period (2015)	Ratio
Precipitation (75 mm)	52 (32, 181)	11 (7, 113)	4.7	Precipitation (119.2 mm)	2508 (677, 64,800)	252 (67, 17,700)	10
TXx (32 °C)	11 (8, 19)	7 (4, 12)	1.6	TXx (34.3 °C)	82 (41, 746)	38 (19, 177)	2.2
TNn (−8 °C)	5 (4, 7)	11 (6, 22)	2.2 *	TNn (−14.6 °C)	192 (111, 426)	529 (246, 1549)	2.8 *

Considering the "moderate" extreme values first, A TXx of 32 °C would have a return period of 11 years (range around these estimates are in Table 7) at the time the actual TXx record was set in 1990 and an equivalent return period of seven years in 2015. A −8 °C TNn event could have been expected once every five years in 1895 but now only once in 11 years in 2015. A 75 mm precipitation event in 1973 would have had a 53-year return period but, once again, could now be expected once every 11 years in the climate of 2015. The global warming influence has altered the ratio between the return times (decreased for TNn) of these records by 1.6 times for TXx, 2.2 times for TNn and 4.7 times for precipitation compared to the year when the actual records were set.

In terms of the actual WP record values, TXx had a return value of 82 years, TNn 192 and precipitation 2508. The return values for TXx and precipitation, under the influence of a warming climate, have been reduced to 38 (TXx) and 252 (precipitation) years and increased to 529 years for TNn which represent ratios in return periods of 2.2 (TXx), 2.8 (TNn) and 10 (precipitation). We wish to clarify that there are large uncertainties associated with extreme value analysis and the results presented for the WP record values must be interpreted with caution. There are the large intervals around precipitation return periods, which in general should not be estimated for periods longer than four times the length of the time series [25]. However, the values given in Table 7 reflect the fact that the 1973 precipitation record was indeed exceptional in the WP record and any extreme value fit will struggle to accurately constrain this (when a single large outlier is so far from the centre of the distribution). To answer our initial question (concerning the probability of event occurrence and a global warming influence), regardless of how much faith is placed in the exact quantitative estimate of the return time of the WP records, the observed pattern is that the global warming influence (as a covariate in determining the location and/or scale parameter of the extreme value distribution) serves to reduce (increase) the return period associated with extreme warm (extreme cold) temperatures and precipitation.

3.3. Climate Model Analysis

Two extreme indices, TXx and RX1Day were chosen for analysis alongside mean TX and precipitation from Coupled Model Intercomparison Phase 5 (CMIP5) output. These two societally-relevant indices were chosen as best representing high impact temperature and precipitation events. We obtained monthly mean TX and precipitation data from the CORDEX ensemble [26] held on the Climate Explorer website (https://climexp.knmi.nl/start.cgi) for 41 European-domain regional climate model runs at 0.5° resolution (forced by CMIP5 model runs). In addition, we obtained daily TX and precipitation data from the 0.25° resolution, statistically-downscaled dataset from NASA Earth Exchange (NEX, [27]). From these two archives (Supplementary B), we extract the grid box closest to WP from each model and use this to assess future climate changes in mean annual (CORDEX and NEX) and extreme (NEX) temperature and precipitation. We compare the historical base period of 1951–2005 with three future periods; a 1.5 °C and 2 °C above pre-industrial world and the 2080–2099 end of 21st century conditions. Our selection of these periods is based on the 2015 Paris agreement to limit global warming to 2 °C above pre-industrial temperatures and to attempt to limit the warming to 1.5 °C [28]. We define 1.5 and 2 degree worlds as the years from future climate projections where the 15-year global average near-surface air temperature is between 1.4–1.6 °C (for a 1.5 °C world) and 1.9–2.1 °C (for a 2 °C world) above the average temperature of the historical 1861–1890 period for each model. Under Representative Concentration Pathway 8.5 (RCP8.5)—the most severe of four warming scenarios used in the CMIP5 projections and the forcing scenario used in the 21 NEX model outputs that we analyse—a 1.5 °C world with our definition can appear as early as 2006 (late as 2048) with a mean year of 2024 and a 2 °C world as soon as 2021 (late as 2061) with a mean year of 2039.

Figure 6 presents histograms of the 1951–2005 mean for Weston Park and the CORDEX/NEX model ensembles for: (a) mean TX; (b) TXx; (c) mean Precipitation; and (d) RX1Day. Histograms for the 1.5/2 °C worlds are presented as well as the end of 21st century period. Data are presented as anomalies relative to the 1951–2005 period (and as per cent anomalies for precipitation), with the figure

replicated using absolute values in the supplementary material (Figures S2 and S3). Beginning with mean TX (Figure 6a) we show that the range of values in the base period is comparable between WP and the CORDEX/NEX ensembles, with the whiskers (1.5 times the inter-quartile range) of all three box plots all ~±1.5 °C. A 1.5/2 °C warmer world shifts the TX distribution upward by ~1 °C with NEX slightly warmer than CORDEX in both cases. A t-test between the 1.5/2 °C values identifies a significant difference in means of 0.3/0.4 °C for CORDEX and NEX respectively, i.e., a statistical difference between these idealised-worlds. With respect to the 1951–2005 model mean period, CORDEX TX warms 0.9 ± 0.1 °C/1.1 ± 0.1 °C in a 1.5/2 °C world and NEX TX warms 1.0 ± 0.1 °C/1.4 ± 0.1 °C in a 1.5/2 °C world respectively. However, the range of the distributions illustrates that the 1.5 °C and 2 °C worlds are broadly comparable, especially when compared with the end of century RCP8.5 forcing scenario which has a mean TX warming double that of both the 1.5/2 °C world. The pattern is replicated for TXx (Figure 6b). Here, we see that the exceptional TXx record set in 1990 in the WP record appears as an obvious outlier in the historical base period and the NEX ensemble is in good agreement with the WP distribution. Out of the 21 NEX models, 13/1155 years (1951–2005) have a TXx standardised anomaly (we use this metric to account for the differences in variance between the WP record and individual model series) greater than or equal to the standardised TXx anomaly of the 1990 WP record, which gives an approximate return period of 89 years—comparable to the 82-year return period for TXx for the climate of 1990 in the observational record (Table 7). For model years in the 1.5/2 °C world, the previously unlikely TXx record becomes reachable within the confines of the range of the model distribution and such an anomaly (5.8 °C) is almost the median value in model years by the end of the century under RCP8.5. The model mean TXx response in the 1.5 °C world (1.6 ± 0.3 °C) is not statistically distinguishable from that of the 2 °C world (1.9 ± 0.6 °C) but the 2080–2099 period is significantly warmer (5.7 ± 0.3 °C).

For mean annual precipitation (Figure 6c), the WP values deviate around the mean by ~±30%, with the models achieving a similar range but with outliers up to ~±50%. There is a small increase (<10%) in precipitation across all scenarios but robust projections are difficult as variability in precipitation estimates are large and increase for some scenarios. For RX1Day, the record 1973 event (Table 2) is not exceeded under any scenario even by outlier events, indicating the exceptional nature of the 1973 event (or a model deficiency in simulating extreme precipitation which is discussed in Section 4.2). The shifts in mean for each scenario here are more pronounced than for mean precipitation. The shift in model mean for RX1Day associated with a 1.5/2 °C world is 7.5% ± 3.5%/10.2% ± 5.1% respectively, with a t-test indicating the 1.5/2 °C worlds do not have statistically different means. The expected RX1Day increase by 2080–2099 is 18.5% ± 15.8%. We discuss the implications and validity of these predictions in Section 4.2.

To place the changes at WP into a wider context, we average all available 1.5/2 °C world model years and plot the ensemble difference in Figure 7. The patterns in mean TX and precipitation follow expected climate warming patterns—Arctic Amplification, continents warmer than oceans, less warming in the central North Atlantic Ocean (Figure 7a) and enhancement of existing precipitation/evaporation patterns (Figure 7e). There are some marked contrasts between the 2 °C and 1.5 °C world in TXx (Figure 7c). In the ensemble analysed here, the difference between 1.5/2 °C shows up very strongly in Arctic Sea Ice regions and suggests a pronounced land-ocean contrast in TXx differences. Changes in RX1day are noisy but broadly reflect the mean precipitation pattern. In a similar way to Figure 1, the location of WP in the centre of the UK located in a somewhat transitional zone when considering the 1.5/2 °C world differences. The central UK mean TX is warmer but TXx does not change much for the north of the UK (Figure 7b,d), and the main precipitation intensification is across the west coast (Figure 7f,h).

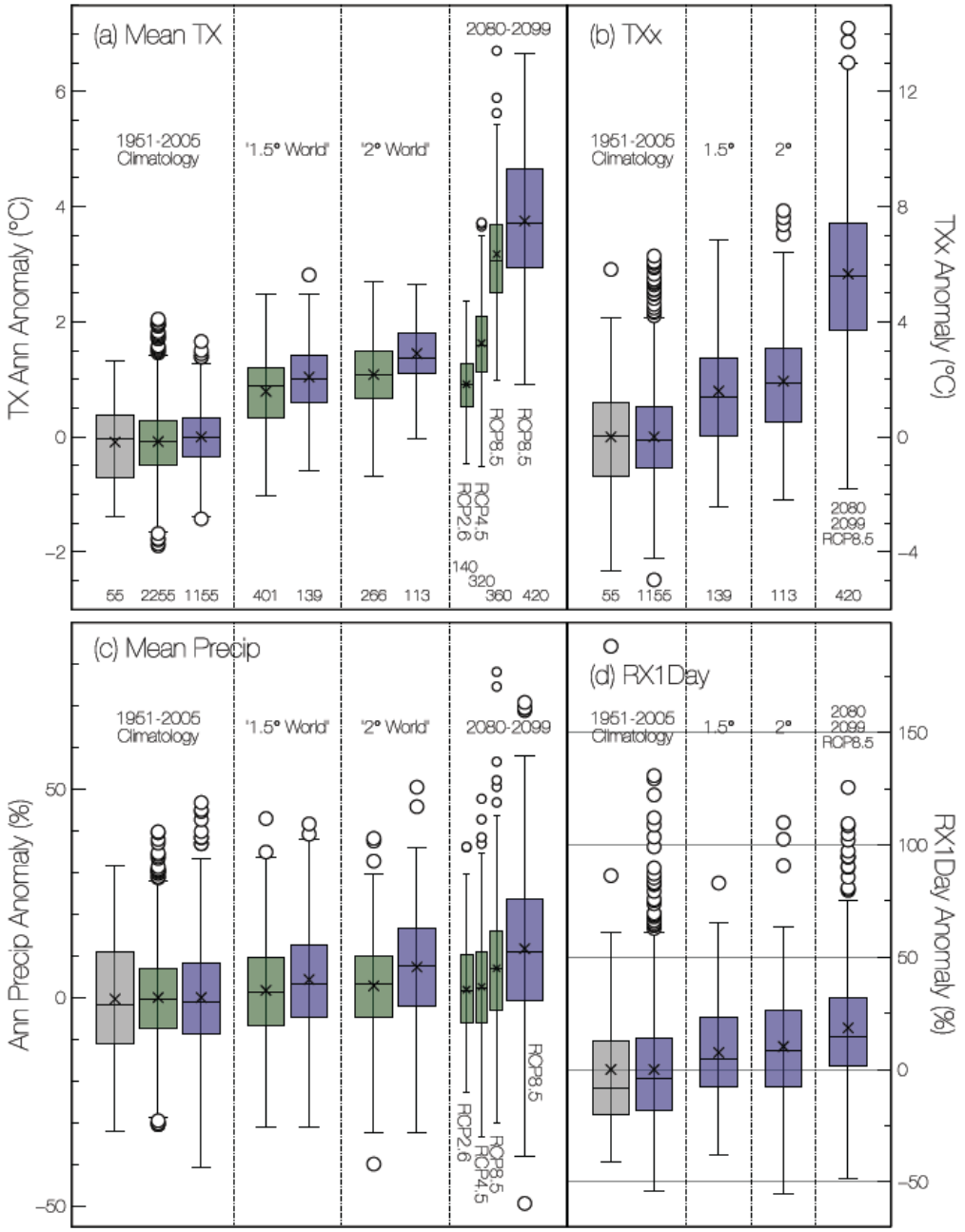

Figure 6. Histograms of WP station data (grey shading), CORDEX (green shading) and NEX (blue shading) climate model output for: (**a**,**b**) annual mean TX and TXx; and (**c**,**d**) annual total precipitation and RX1Day. All data are presented as anomalies (per cent for precipitation) relative to the 1951–2005 mean for each index (station mean data for WP, an individual model data for CORDEX/NEX). Numbers along the upper x-axis indicate the number of available years of data contributing to each histogram. Four time periods are analysed: the historical/base period 1951–2005, model results from when global temperatures are in a 1.5/2 °C world (defined in the main text) and for the end of 21st century period 2080–2099. The 2080–2099 CORDEX box plots are split via RCP scenarios. An alternative version of this figure showing absolute magnitudes is in the supplementary material.

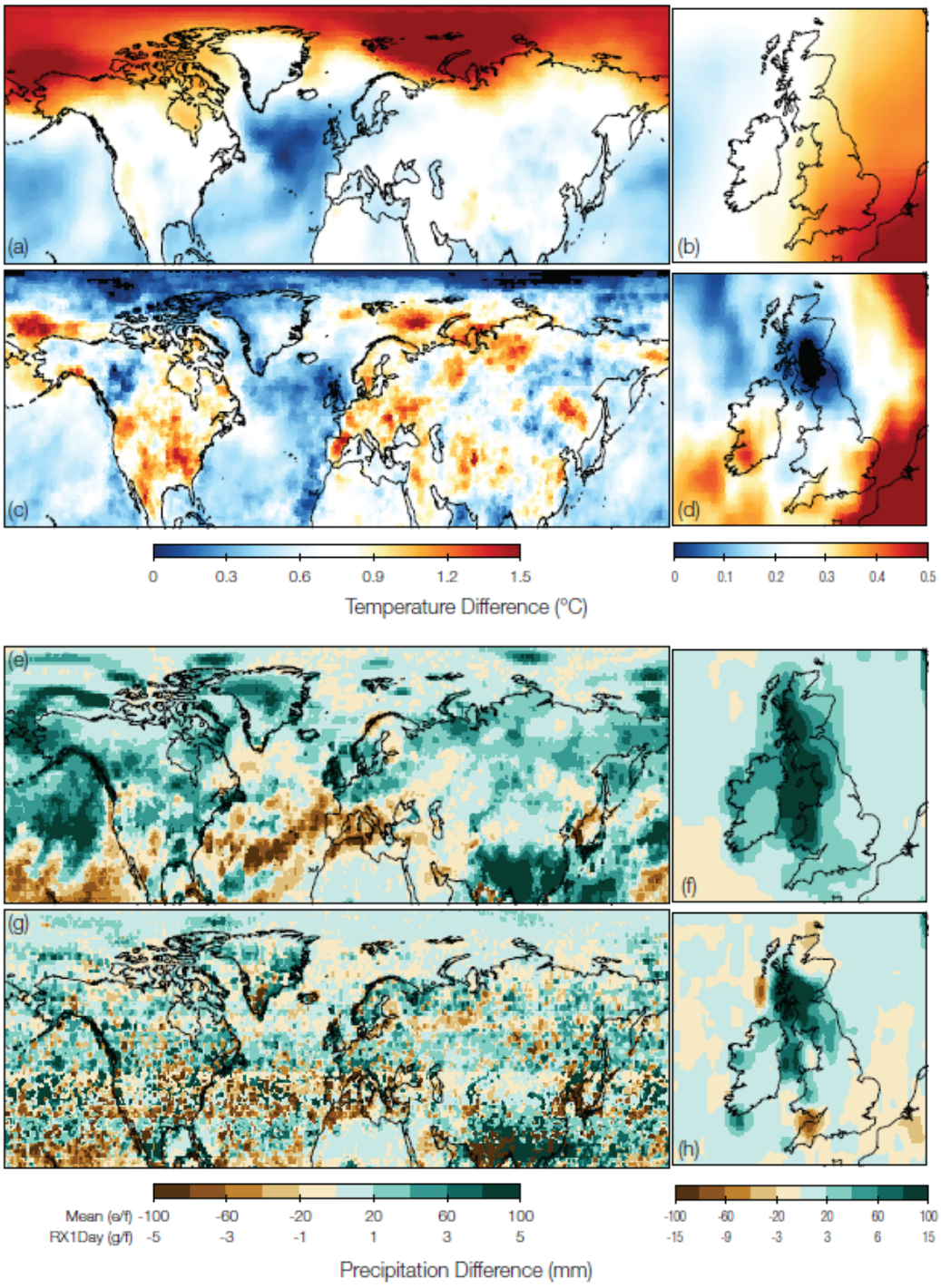

Figure 7. The composite difference between the 2 °C and 1.5 °C above pre-industrial worlds (the ensemble mean of all model years for the years which qualified as a 1.5/2 °C world using our criteria) for: (**a**,**b**) TX; (**c**,**d**) TXx; (**e**,**f**) annual mean precipitation; and (**g**,**h**) RX1Day.

To return to the second of our two questions, will current climate records become "normal"? Whilst we have not analysed model minimum temperatures, the general shift in the temperature distribution makes it extremely unlike the TNn record will be surpassed (Table 7). The TXx record is within the range of the model distribution in a 1.5/2 °C world and what constitutes the record value in the climate of 2015 would be about the median expected TXx value at the end of the 21st century under

RCP8.5 forcing. The record RX1Day value is not exceeded at all in any simulation and its exceptional nature within the existing WP record suggests it is unlikely such a record will be easily surpassed.

3.4. Circulation and Climate Indices

Figure 8 presents a correlation matrix between various climate indices and WP seasonal mean and extreme indices from 1979–2015. We comment on the consistent correlations here (i.e., that show up in numerous seasonal indices) that are analysed in the discussion (Section 4.3), although as Figure 8 shows there are some isolated significant correlations (which would be expected when testing many samples due to chance) that we do not discuss. The North Atlantic Oscillation (NAO) and Arctic Oscillation (AO) significantly correlate with most temperature indices in winter and spring, with the Greenland Blocking Index (GBI) and Scandinavian pattern (SCAND) mirroring these trends but with the opposite sign. The East Atlantic pattern (EA) correlates significantly with winter precipitation indices and autumn temperatures, and the East Atlantic-Western Russian (EA-WR) pattern correlates significantly with mean spring temperatures. In summer, the Principal Component-based NAO and AO correlate positively with TX indices and DTR, and negatively with precipitation indices, again with the patterns reversed for the GBI. An additional significant correlation of note is autumn sea ice with mean temperature indices. A version of Figure 8 using detrended anomalies is provided in the Supplementary Materials (Figure S4), which does not affect the results.

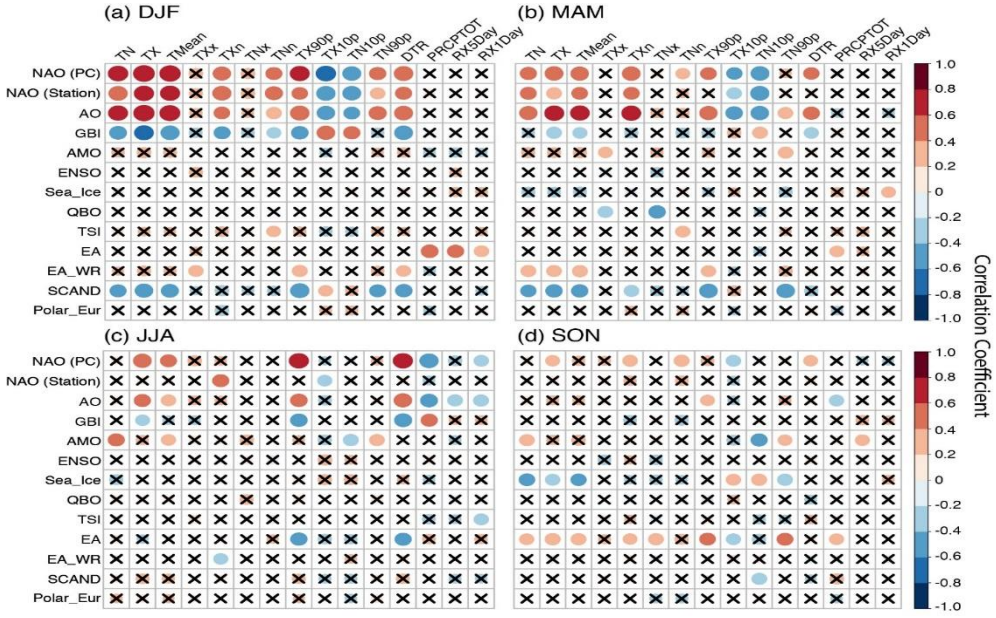

Figure 8. Seasonal correlation coefficients (1979–2015) between WP climate indices (mean temperature, TX/TN and ETCCDI indices from Table 1) and selected climate indices. Insignificant correlations ($p > 0.05$) are marked with a black cross. (**a**) DJF. (**b**) MAM. (**c**) JJA. (**d**) SON. NAO, North Atlantic Oscillation (principal component and station-based); AO, Arctic Oscillation; GBI, Greenland Blocking Index; AMO, Atlantic Multidecadal Oscillation; ENSO, Multivariate El Niño Southern Oscillation Index; Sea_Ice, Arctic Sea Ice extent; QBO, Quasi-biennial Oscillation at 30 hPa; TSI, Total Solar Irradiance; EA, East Atlantic pattern; EA-WR, East Atlantic–Western Russian pattern; SCAND, Scandinavian pattern; Polar_Eur, Polar-Eurasian pattern. Data sources are listed in Supplementary C.

4. Discussion

4.1. Historical Trends in Mean and Extreme Climate

Trend analysis indicates that annual mean WP temperature and precipitation increased at a significant rate of 1.0 °C/69 mm century^{-1} between 1883 and 2015 (Table 5). This is coherent with

an overriding anthropogenically-forced climate warming signal [29]. Whilst the WP station has not moved more than a few metres in its location throughout its operation and the population of Sheffield has stayed reasonably constant through the past 100-years [30], it is assumed that 20th century urbanisation could add a small Urban Heat Island contribution to the long term warming trend. There is multi-decadal variability in the seasonal and temporal trends, including a (non-significant) negative temperature trend widespread across all mean temperature trends during 1941–1970, mirroring the cooling in global average temperatures across this period, which is associated with anthropogenic aerosols dominating the (particularly Northern Hemisphere) climate forcing at this time [31]. Outside of centennial and recent 30-year periods (1971–2000 and 1981–2010), significant trends in temperature are typically lacking. This is also the case with mean precipitation, with no significant trends in the time series outside of the annual long term trend and for autumn (1941–1970). This reflects the greater variability in a local climate record as opposed to a regional/hemispheric/global trend, which provides a weaker signal-to-noise ratio than spatially averaged records.

Since the turn of the 21st century, December 2010 and March 2013 are the only two months to register a cold record (Table 4), both of which were associated with exceptionally negative NAO conditions [6,32]. There have also been two record wet (2002 and 2012) and dry (2003 and 2011) years since the turn of the century which again illustrates the importance of natural variability in the WP record which, like for the wider-European region as well, arises due to subtle changes in the polar front jet stream [33].

The general weather pattern that is related to higher summer precipitation across the UK is that of a negative NAO/positive GBI [17]. A positive GBI index implies strong blocking conditions above Greenland, which leads to a southerly migration and sometimes north/south splitting of the jet stream with resulting increased precipitation over the UK. There has been a significant increase (decrease) in the GBI (NAO) in summer since about 1990 [17,18]. The GBI/NAO-precipitation relationship is identified in our correlation analysis (Figure 8) and is a likely contributing factor in the increasing (but not significant) WP summer 1981–2010 and 1991–2015 precipitation trend (Table 5) and also the three (two) record June (summer) precipitation values. The enhanced loss of Arctic sea ice since 2007 is a potential driving mechanism that favours a southerly displaced jet stream [3] and Greenland Blocking [34].

Trends in extreme indices (Figure 4; Table 6) vary in magnitude but mirror the long term mean warming and wetting trends. Out of the four temperature percentile-based indices, TX90p ("warm days") has a weaker trend (4% century^{-1}) across the entire record than the three related (TN10p, TX10p and TN90p) indices (5%–7% century^{-1}) and also is the only non-significant trend out of the temperature percentile-based indices for the 1981–2010 period, which coincides with only one TXx record set since 1990 (Table 2). Additionally, TR15 trends from 1883–2015 are double that of SU25. Across Europe, northerly winds (and associated cold days) are warming at a faster rate than southerly winds (and associated warm days [35]) which can explain why colder conditions are warming at a faster rate at WP. In addition, the shallower planetary boundary layer at night time is more responsive to greenhouse gas induced warming [36], which can also offer an explanation for greater warming rates for the "cold" extreme indices. The DTR trend reflects this (negative trend throughout 1981–2010 and 1991–2015) but it is not statistically significant. The preponderance of the negative summer NAO state in the recent past [18] favours conditions unsuitable for higher (i.e., summer daytime maximum) temperatures, whereas the positive summer NAO, favouring blocking conditions over the UK would favour higher summer temperatures. These factors may explain the relatively lower trend rate in TX90p and also, the non-significant yet decreasing trend in summer TX (Table 5) for the 1991–2015 period (-0.09 °C·decade^{-1}), which is opposite to the significantly increasing long term 1883–2015 trend (1.06 °C·century^{-1}).

Precipitation at WP has increased across all seasons during 1883–2015 (Table 5). There are no significant changes in wetness/dryness metrics (CWD/CDD) but SDII—a measure of precipitation amount on wet days only—has significantly increased (Table 6, Figure 4), as such we can surmise

that precipitation intensity has increased and precipitation frequency has not changed. With a total of 58 days (19 more than the second highest value shared between 1915, 1947 and 1957), the CDD index value in 1959 stands out remarkably in the time-series (Figure 4). An attribution analysis is beyond the scope of this paper; however, we note that the 1959 drought, which affected over ten million people, is the most severe UK national scale drought in independent 229- and 63-year drought indices and not localised to WP [37,38].

4.2. Future Evolution of Extremes

Analysis of climate model output indicates that the main difference for WP between a 1.5 °C and 2 °C above pre-industrial world is a significant difference in mean TX but not in mean precipitation, TXx or RX1Day. There is a significant difference between either the 1.5 °C and/or 2 °C world and the 2080–2099 end of century RCP8.5 forced period in all analysed parameters. The WP record TXx value is rarely exceeded (~88 year return period) in the historical 1951–2005 climate period but is well inside the model range of both 1.5/2 °C worlds, and the mean shift in this variable between the end of 21st century and model historical mean is 5.8 °C, with values able to go above 12 °C (Figure 6b). Changes in RX1Day in the 1.5/2 °C world are ~8%–10% and ~18% by the end of the 21st century but model ranges are large. Not a single model we analysed displayed an RX1Day value above the 1973 WP record (Table 2), even by the end of the 21st century under strong anthropogenic forcing. Combined with extreme value analysis of the WP record (Table 7), this indicates a remarkably exceptional event.

At the hemispheric-scale, our ensemble difference between the 1.5 °C and 2 °C world highlights a strong difference in TXx over the Barents-Kara-Laptev and Bering seas in the Arctic (Figure 7c), implying a 2 °C threshold for significant Arctic Sea Ice loss in these regions. Northern Hemisphere continents, particularly continental Europe and Central America, display a pronounced difference between the 1.5 °C/2 °C worlds. This result is important with respect to future endeavours to limit global warming to 1.5 °C above pre-industrial conditions as it shows a difference between 1.5 °C/2 °C worlds that is more important to humans, i.e., extreme temperatures, which have a greater impact than subtle shifts in the mean. The mean warming is strongest over the Arctic, which, whilst important for the planet, is not where many humans inhabit, whereas here we see that the populous zones of continental Europe and North America would be most strongly impacted by TXx changes in a 2 °C relative to a 1.5 °C world. This analysis was not the major focus of this study and we use only 21 climate models, as such, studies which examine the 1.5/2 °C world difference in more climate metrics should be pursued with large ensembles (medium forcing scenarios would be advantageous to give more 1.5 °C and 2 °C available years than the rapidly warming RCP8.5 scenario). These general observations relate to a recent study by Huntingford and Mercado [39] who showed that land regions will experience higher global warming based impacts as they warm at a ratio ~1.5 that of the oceans.

The projected increase in extreme temperature and precipitation is expected under the thermodynamic response to anthropogenically forced warming, i.e., higher temperatures and Clausius-Clapeyron temperature-precipitation scaling. However, the near- and long-term evolution of dynamics/circulation, which could be forced by natural/random variability, as well as by anthropogenic forcing, could have just as strong an effect as the thermodynamic anthropogenic signal and either augment or counter the global warming influence [40]. As Figure 5 shows, the daily record TXx/TNn/precipitation values occur under certain conditions. If either of these preferred patterns occur with increased frequency (summer anticyclones for TXx, anomalous easterly jet/NAO- for TNn and (typically summer) cyclones for precipitation)) then future trends in extremes might be less or greater than expected. The exception is for cold extremes, which are likely to be less severe due to global warming, evidenced by the fact that only two cold month records have been set at WP since the turn of the 21st century (Table 4) and both of these cases were associated with exceptionally negative monthly NAO indices.

Figure 5 illustrates that WP daily precipitation record totals occur during summer cyclone conditions with a likely contribution from convective enhancement, rather than convection serving

as the dominant mechanism which would be expected in the warmer southern UK [41]. Extreme precipitation is expected to roughly scale with temperature at 7% $^{\circ}C^{-1}$. Berg et al. [42] showed that for frontal precipitation, this relationship broadly holds true, but for convective precipitation, the scaling factor can be exceeded. Global climate models are of insufficient resolution to resolve convection, which has been shown to lead to lower sub-daily precipitation intensities compared to a model run at weather-forecast resolution ("convection permitting") across the southern UK [41]. This implies that future estimates of extreme precipitation in a warmer world may be underestimated in current generation global climate models. However, Hawcroft et al. [43] showed that >70% of winter and summer precipitation across the UK was due to frontal precipitation, which global climate models simulate well in terms of frequency and precipitation amount [44], so the predictions for WP regarding RX1Day (Figure 6) may be better constrained than they would be for southerly latitude locations where convection-dominated precipitation is more common, although the range of predictions is still wide (in this study and in the mid-latitudes in general) due to uncertainties in atmospheric circulation changes [29,45,46]. Given that WP is centred on the boundary between the climatologically wetter northwest and drier southeast, subtle changes in the orientation of the storm tracks will likely be the more dominant driver in extreme precipitation changes than the smaller, but more robust (~8%–10% at WP for a 1.5/2 °C world) expected increase due to Clausius-Clapeyron scaling. Conversely, moisture availability may be a limiting factor in future extreme precipitation events [45]. In addition, we have not discussed the potential influence of the Pennine Mountains to the west of Sheffield in influencing precipitation by orographic enhancement. A warmer climate might result in a shift of precipitation downwind in orographic regions [47]. Many storms that cross the UK do so from the southwest, so this factor could enhance precipitation rates across WP and rain-shadow regions of the UK.

4.3. Links with Climate Indices

This correlation analysis (Figure 8) provides a basic metric of the approximate state of the atmosphere/ocean (through whichever climate index) and WP data at the same point in time and does not take into account temporal lags and the various physical pathways by which climate modes of variability can influence different parts of the world. As such, whilst Figure 8 does not discount the influence of the climate modes that show non-significant correlations, we can still comment on significant correlations that do occur and are of interest (Section 3.4). Firstly, the NAO and AO have a strong positive correlation with winter and spring mean and extreme temperature indices (anti-correlation with the 10th percentile extreme indices) but the EA pattern better correlates with precipitation total and the RX1/5Day index. The NAO (AO) and EA essentially are both indices of the zonal flow into Western Europe (both have a south-north dipole) with the EA a more "south-east-shifted" version of the NAO which is related to the direction and orientation of westerly storms into Europe. Supplementary Figure S5 highlights the difference between the NAO and EA in terms of winter correlations with mean temperature and precipitation and shows that for WP, the EA is a better indicator of storms that result in precipitation at WP (central England) than the NAO, which has significant correlations across the western coastlines of the UK and Ireland, indicating a more north-easterly storm track. This lends credence to the idea that more relevant jet-stream indicators [33,48] than that of a one-dimensional index would be useful in explaining climate variations.

The GBI and SCAND pattern display opposite correlations to the NAO and AO. These two patterns are structurally different, with the positive mode of each having a blocking high situated over Greenland or Scandinavia respectively. The relevance for WP here is that a block set up over either of these locations likely results in a (downstream for GBI, upstream for SCAND) southward-shifted jet stream, leading to colder winter UK conditions. The EA-WR positive correlation with mean temperature during spring has been identified as persistent in time across North-western Europe since 1950 [49] and is associated with a blocking pattern centred above the UK which whilst variable in spring, would usually be associated with drier, warmer conditions. The negative sea-ice relationship with temperature in autumn (positive for the 10th percentile temperature indices) is possibly due to

the sea ice loss influencing the jet stream position, although there are multiple competing factors on European (and therefore WP) climate variability [33–35,50].

5. Conclusions

Analysis of WP data indicates a long term (1883–2015) significant annual warming and wetting trend in line with an expected global warming signal. Trends in extreme temperature indices as defined by the ETCCDI mirror the mean warming signal. Precipitation intensity is increasing, evidenced by significant positive trends in the SDII index alongside the setting of four daily precipitation total records since the turn of the 21st century. Global warming has contributed to an increasing likelihood of warm and wet extremes and decreasing likelihood of cold extremes. The significance of weather patterns and their relationship to extremes at WP has been discussed. We find that several climate indices can be relevant in explaining temperature and precipitation variability, with the (N)AO, EA, GBI and SCAND patterns identified as significantly correlating modes of influence. Future evolution of annual extreme hot temperature and heavy precipitation events from climate model output is more drastic by the end of the 21st century compared to our defined 1.5 and 2 degree warmer worlds. As such, societal measures to actively reduce anthropogenic greenhouse forcing (e.g., COP21 [28]), which would keep the future trajectory of the planet below the RCP8.5 scenario and within the realm of a 1.5–2 °C above pre-industrial world, would be beneficial in keeping the climate of WP within somewhat "normal" bounds. The appraisal of long-term historical daily resolution station data in previously under-analysed regions should be continued in order to increase the global assessment of historical and present climate extreme variability.

Supplementary Materials: Supporting text and five supporting figures submitted with the manuscript.

Acknowledgments: We kindly thank Alistair McClean for providing WP weather data and information about the station history and also thank Professor Edward Hanna for reviewing a draft of the manuscript. We also thank the editor for handling the paper and appreciate several helpful comments from three reviewers, which improved the paper. We thank the data providers whose freely available products allowed us to perform the analysis in this paper.

Author Contributions: Both authors were involved in the design, analysis and writing of the paper.

Conflicts of Interest: The authors declare no conflict of interest.

References

1. Blackburn, M.; Methven, J.; Roberts, N. Large-Scale context for the UK floods in summer 2007. *Weather* **2008**, *63*, 280–288.
2. Hanna, E.; Mayes, J.; Beswick, M.; Prior, J.; Wood, L. An analysis of the extreme rainfall in Yorkshire, June 2007, and its rarity. *Weather* **2008**, *63*, 253–260.
3. Screen, J.A. Influence of Arctic sea ice on European summer precipitation. *Environ. Res. Lett.* **2013**. [CrossRef]
4. Kendon, M.; Marsh, T.; Parry, S. The 2010–2012 drought in England and Wales. *Weather* **2013**, *68*, 88–95. [CrossRef]
5. Christidis, N.; Stott, P.A.; Ciaverella, A. The effect of anthropogenic climate change on the cold spring of 2013 in the United Kingdom. *B. Am. Meteorol. Soc.* **2014**, *95*, S79–S82.
6. Prior, J.; Kendon, M. The disruptive snowfalls and very low temperatures of late 2010. *Weather* **2011**, *66*, 315–321. [CrossRef]
7. Prior, J.; Kendon, M. The UK winter of 2009/2010 compared with severe winters of the last 100 years. *Weather* **2011**, *66*, 4–10. [CrossRef]
8. Kendon, M.; McCarthy, M. The UK's wet and stormy winter of 2013/2014. *Weather* **2015**, *70*, 40–47. [CrossRef]
9. Record Breaking Winter for England and Wales. Available online: http://www.metoffice.gov.uk/news/releases/2016/winter-statistics (accessed on 6 may 2016).
10. King, A.D.; Van Oldenborgh, G.J.; Karoly, D.J.; Lewis, S.C.; Cullen, H. Attribution of the record high Central England temperature of 2014 to anthropogenic influences. *Environ. Res. Lett.* **2015**. [CrossRef]
11. Kendon, M. Has there been a recent increase in UK weather records? *Weather* **2014**, *69*, 327–332. [CrossRef]

12. Dee, D.P.; Uppala, S.M.; Simmons, A.J.; Berrisford, P.; Polia, P.; Kobayashi, S.; Andrae, U.; Balmaseda, M.A.; Balsamo, G.; Bauer, P.; et al. The ERA-Interim reanalysis: Configuration and performance of the data assimilation system. *Q. J. R. Meteorol. Soc.* **2011**, *137*, 553–597. [CrossRef]
13. Haylock, M.R.; Hofstra, N.; Klein Tank, A.M.G.; Klok, E.J.; Jones, P.D.; New, M. A European daily high-resolution gridded data set of surface temperature and precipitation for 1950–2006. *J. Geophys. Res.* **2008**. [CrossRef]
14. Weston Park Weather Station. Available online: http://lifeofdata.org.uk/node/weston-park-weather-station/ (accessed on 1 January 2016).
15. RClimDex User Manual. Available online: http://etccdi.pacificclimate.org/software.shtml (accessed on 1 January 2016).
16. Hamed, K.H.; Rao, A. A modified Mann-Kendall trend test for autocorrelated data. *J. Hydrol.* **1998**, *204*, 182–196. [CrossRef]
17. Hanna, E.; Cropper, T.E.; Hall, R.; Cappelen, J. Greenland Blocking Index 1851–2015: A regional climate change signal. *Int. J. Climatol.* **2016**. [CrossRef]
18. Hanna, E.; Cropper, T.E.; Jones, P.D.; Scaife, A.A.; Allan, R. Recent seasonal asymmetric changes in the NAO (a marked summer decline and increased winter variability) and associated changes in the AO and Greenland Blocking Index. *Int. J. Climatol.* **2015**, *35*, 2540–2554. [CrossRef]
19. Roger, K.; Hallock, K.F. Quantile regression. *J. Econ. Perspect.* **2001**, *15*, 143–156.
20. 20th Century Reanalysis Daily Composites. Available online: http://www.esrl.noaa.gov/psd/cgi-bin/data/composites/plot20thc.day.v2.pl (accessed on 1 March 2016).
21. Schaller, N.; Kay, A.; Lamb, R.; Massey, N.; van Oldenborgh, G.; Otto, F.; Sparrow, S.; Vautard, R.; Yiou, P.; Ashpole, I.; et al. Human influence on climate in the 2014 southern England winter floods and their impacts. *Nat. Clim. Chang.* **2016**, *6*, 627–634. [CrossRef]
22. Easterling, D.R.; Kunel, K.E.; Wehner, M.F.; Sun, L. Detection and attribution of climate extremes in the observed record. *Weather Clim. Extremes* **2016**, *11*, 17–27. [CrossRef]
23. Siswanto; van Oldenborgh, G.J.; van der Schrier, G.; Lenderink, G.; van den Hurk, B. Trends in high-daily precipitation events in Jakarta and the flooding of January 2014. *Bull. Am. Met. Soc.* **2015**, *96*, 12.
24. Stott, P.; Christidis, N.; Otto, F.; Sun, Y.; Vanderlinden, J.; van Oldenborgh, G.; Vautard, R.; von Storch, H.; Walton, P.; Yiou, P.; et al. Attribution of extreme weather and climate-related events. *Wiley Interdiscip. Rev.: Clim. Chang.* **2016**, *7*, 23–41. [CrossRef] [PubMed]
25. Venäläinen, A.; Saku, S.; Jylhä, K.; Nikulin, G.; Kjellström, E.; Bärring, L. Extremes Temperatures and Enthalpy in Finland and Sweden in a Changing Climate. NKS-194. 2009. Available online: http://www.nks.org/download/pdf/NKS-Pub/NKS-194.pdf (accessed on 18 August 2016).
26. Giorgi, A.; Jones, F.; Asrar, G.R. Addressing climate information needs at the regional level: The CORDEX framework. *WMO Bull.* **2009**, *58*, 175–183.
27. Thrasher, B.; Maurer, E.P.; McKellar, C.; Duffy, P.B. Technical Note: Bias correcting climate model simulated daily temperature extremes with quantile mapping. *Hydrol. Earth Syst. Sci.* **2012**, *16*, 3309–3314. [CrossRef]
28. UNFCCC. Adoption of the Paris Agreement. Proposal by the President. Draft decision CP.21. 2015. Available online: https://unfccc.int/resource/docs/2015/cop21/eng/l09r01.pdf (accessed on 16 August 2016).
29. Stocker, T.F.; Qin, D.; Plattner, G.-K.; Tignor, M.M.B.; Allen, S.K.; Boschung, J.; Nauels, A.; Xia, Y.; Bex, V.; Midgley, P.M. *Climate Change 2013: The Physical Science Basis*; Cambridge University Press: Cambridge, UK, 2013.
30. Sheffield Population Statistics: 1086–2001. Available online: https://www.sheffield.gov.uk/libraries/archives-and-local-studies/research-guides/population-statistics.html (accessed on 6 May 2016).
31. Meehl, G.A.; Washington, W.M.; Ammann, C.M.; Arblaster, J.M.; Wigley, T.M.L.; Tebaldi, C. Combinations of natural and anthropogenic forcings in twentieth-century climate. *J. Clim.* **2004**, *17*, 3721–3727. [CrossRef]
32. Burgess, M.L.; Klingaman, N.P. Atmospheric circulation patterns associated with extreme cold winters in the UK. *Weather* **2015**, *70*, 211–217. [CrossRef]
33. Hall, R.; Erdélyi, R.; Hanna, E.; Jones, J.M.; Scaife, A.A. Drivers of North Atlantic Polar front jet stream variability. *Int. J. Climatol.* **2015**, *35*, 1697–1720. [CrossRef]
34. Liu, J.; Chen, Z.; Francis, J.; Song, M.; Mote, T.; Hu, Y. Has Arctic sea-ice loss contributed to increased surface melting of the Greenland ice sheet? *J. Clim.* **2016**. [CrossRef]

35. Screen, J.A. Arctic amplification decreases temperature variance in northern mid- to high-latitudes. *Nat. Clim. Chang.* **2014**, *4*, 577–582. [CrossRef]
36. Davy, R.; Esau, I.; Chernokulsky, A.; Outten, S.; Zilitinkevich, S. Diurnal asymmetry to the observed global warming. *Int J. Climatol.* **2016**. [CrossRef]
37. Spinoni, J.; Naumann, G.; Vogt, J.V.; Barbosa, P. The biggest drought events in Europe from 1950 to 2012. *J. Hydrol. Reg. Stud.* **2015**, *3*, 509–524. [CrossRef]
38. Marsh, T.; Cole, G.; Wilby, R. Major droughts in England and Wales, 1800–2006. *Weather* **2007**, *62*, 87–93. [CrossRef]
39. Huntingford, C.; Mercado, L.M. High chance that current atmospheric greenhouse concentrations commit to warmings greater than 1.5 °C over land. *Nat. Sci. Rep.* **2016**, *6*. [CrossRef] [PubMed]
40. Collins, M.; Knutti, R. Long-Term climate change: Projections, commitments and irreversibility. In *Climate Change 2013: The Physical Science Basis*; Cambridge University Press: Cambridge, UK, 2013; pp. 1029–1136.
41. Kendon, E.J.; Roberts, N.M.; Fowler, H.J.; Roberts, M.J.; Chan, S.C.; Senior, C.A. Heavier summer downpours with climate change revealed by weather forecast resolution model. *Nat. Clim. Chang.* **2014**, *4*, 570–576. [CrossRef]
42. Berg, P.; Moseley, C.; Haerter, J. Strong increase in convective precipitation in response to higher temperatures. *Nat. Geosci.* **2013**, *6*, 181–185. [CrossRef]
43. Hawcroft, M.; Shaffrey, L.; Hodges, K.; Dacre, H. How much Northern Hemisphere precipitation is associated with extratropical cyclones? *Geophys. Res. Lett.* **2012**, *39*, L24809. [CrossRef]
44. Canto, J.L.; Jakob, C.; Nicholls, N. Can the CMIP5 models represent winter frontal precipitation? *Geophys. Res. Lett.* **2015**, *42*, 8596–8604.
45. Trenberth, K. Changes in precipitation with climate change. *Clim. Res.* **2011**, *47*, 123–138. [CrossRef]
46. Shepherd, T.G. Atmospheric circulation as a source of uncertainty in climate change projections. *Nat. Geosci.* **2014**, *7*, 703–708. [CrossRef]
47. Siler, N.; Roe, G. How will orographic precipitation respond to surface warming? An idealized thermodynamic perspective. *Geophys. Res. Lett.* **2014**, *41*, 2606–2613. [CrossRef]
48. Gillett, N.P.; Fyfe, J.C. Annular mode changes in the CMIP5 simulations. *Geophys. Res. Lett.* **2013**, *40*, 1189–1193. [CrossRef]
49. Ionita, M. The impact of the East Atlantic/Western Russia pattern on the hydroclimatology of Europe from Mid-Winter to late Spring. *Climate* **2014**, *2*, 296–309. [CrossRef]
50. Overland, J.E.; Francis, J.A.; Hall, R.; Hanna, E.; Kim, S.-J.; Vihma, T. The melting Arctic and mid-latitude weather patterns: Are they connected? *J. Climat.* **2015**, *28*, 7917–7932. [CrossRef]